

Chaos-based reinforcement learning with TD3

Toshitaka Matsuki^{a,*}, Yusuke Sakemi^{b,c}, Kazuyuki Aihara^{b,c}

^a*National Defense Academy of Japan, Kanagawa, Japan*

^b*Research Center for Mathematical Engineering, Chiba Institute of Technology, Narashino, Japan*

^c*International Research Center for Neuro intelligence (WPI-IRCIN), The University of Tokyo, Tokyo, Japan*

Abstract

Chaos-based reinforcement learning (CBRL) is a method in which the agent's internal chaotic dynamics drives exploration. This approach offers a model for considering how the biological brain can create variability in its behavior and learn in an exploratory manner. At the same time, it is a learning model that has the ability to automatically switch between exploration and exploitation modes and the potential to realize higher explorations that reflect what it has learned so far. However, the learning algorithms in CBRL have not been well-established in previous studies and have yet to incorporate recent advances in reinforcement learning. This study introduced Twin Delayed Deep Deterministic Policy Gradients (TD3), which is one of the state-of-the-art deep reinforcement learning algorithms that can treat deterministic and continuous action spaces, to CBRL. The validation results provide several insights. First, TD3 works as a learning algorithm for CBRL in a simple goal-reaching task. Second, CBRL agents with TD3 can autonomously suppress their exploratory behavior as learning progresses and resume exploration when the environment changes. Finally, examining the effect of the agent's chaoticity on learning shows that extremely strong chaos negatively impacts the flexible switching between exploration and exploitation.

Keywords: chaos-based reinforcement learning, TD3, echo state network

1. Introduction

Neural networks (NNs) have been studied for many years, partially inspired by findings in neuroscience research [1]. In recent years, the development of deep learning techniques used to successfully train deep NNs has produced remarkable results in various machine learning fields. The recent progress in this field began with outstanding achievements in the study of image recognition with NNs [2, 3, 4]. Recurrent neural networks (RNNs) also performed well in time-series processing, such as speech recognition and natural language processing [5, 6, 7, 8]. Vaswani et al. proposed the transformer, which is an innovative model for natural language processing [9]. The transformer has

*Corresponding author

Email address: t_matsuki@nda.ac.jp (Toshitaka Matsuki)

provided a breakthrough in the capabilities of artificial intelligence (AI) as the underlying technology for Large Language Models (LLMs) [10]. It has also demonstrated high performance in other areas such as image processing and speech recognition [11, 12]. AI capabilities based on deep learning techniques have developed quickly over the past decade, leading to innovations in diverse fields.

In recent years, AI has demonstrated even high-quality creative abilities [13], and the creativity of AI has been attracting much attention [14, 15]. The outputs of LLMs can be made more conservative or more creative by modifying a probability distribution parameter called “temperature” [16]. Historically, J. McCarthy et al. discussed the difference between creative thinking and unimaginative competent thinking in a proposal for the Dartmouth Workshop in 1956 [17]. They raised the importance of randomness in AI and the need to pursue how randomness can be effectively injected into machines, just as the brain does. In reinforcement learning, a learning agent performs exploratory action driven by random numbers to an environment and improves its policy based on feedback from the environment. Reinforcement learning is inspired by psychological findings and the principle of reinforcement, which states that agents learn from their actions and their consequences. Various studies on reinforcement learning have been conducted over long years [18, 19, 20, 21, 22, 23]. In recent years, research on deep reinforcement learning, which incorporates deep learning techniques, has become popular, and this approach has made it possible to learn even more difficult tasks [24, 25, 26, 27, 28]. Deep reinforcement learning can also provide effective learning performance in tasks such as Go and video games, where it is difficult to specify the desired behavior designed by human hands [29, 30, 31]. Randomness enables AI systems to generate creative outputs and perform exploratory learning.

This study focuses on the spontaneous and autonomous exploration of organisms. Organisms can act spontaneously and autonomously in environments with diverse dynamics, and can adapt to the environment based on the experience gained through these behavior [18]. Reinforcement learning agents stochastically explore the environment by introducing random numbers to select actions that deviate from the optimal action determined by the current policy. On the other hand, it remains a fascinating unsolved problem to understand how the biological brain behaves in various ways and realizes exploratory learning. One hypothesis for the essential property of the source of exploration is to utilize fluctuations within the brain. Various studies have shown that fluctuations caused by spontaneous background activity in the neural populations vary their responses [32]. Briggman et al. demonstrated that decision-making of escape behavior in leeches depends on the activity of specific neurons that fluctuate under the influence of neuronal population dynamics [33]. Fox et al. measured activity in the human motor cortex with fMRI while performing a button-pressing task, and they found a correlation between fluctuations in the BOLD signals and behavioral variability [34]. These studies suggest that fluctuations in neural activity influence decision-making and produce a variety of behaviors.

Freeman pointed out the possibility that the brain uses chaotic dynamics for exploratory learning [35]. Skarda and Freeman observed the EEG of the rabbit olfactory system and showed that there are many chaotic attractors in the dynamics of the olfactory bulb that are attracted when the rabbit is exposed to the known olfactory conditioned stimulus [36]. This study has also confirmed that when the rabbit is exposed to an unknown odorant, chaotic dynamics that itinerate between existing attractors emerge,

followed by the reorganization of existing attractors and the emergence of new attractors corresponding to new stimuli. Freeman argues that the chaotic dynamics of the brain continually generate new patterns of activity necessary to generate new structures and that this underlies the ability of trial and error problem solving [35]. Aihara et al. discovered the chaotic dynamics in the squid giant axon and constructed chaotic neural network models based [37, 38, 39], and proposed Chaotic Simulated Annealing effective for combinatorial optimization problems [40]. Hoerzer et al. showed that a reservoir network, which fixes the recurrent and input weights, can acquire various functions using an exploratory learning algorithm based on random noise [41]. This study examined how generic neural circuits that resemble a cortical column can acquire and maintain computational functions, including memory attractors, through biologically plausible learning rules rather than supervised learning. The result suggests that stochasticity (trial-to-trial variability) of neuronal response plays a crucial role in the learning process. It has also been shown that the system’s own chaotic dynamics can drive exploration in this learning process [42, 43]. These studies have implications for understanding how the brain achieves exploratory learning and utilizes chaotic dynamics in the process.

Shibata et al. have proposed chaos-based reinforcement learning (CBRL), which exploits the internal chaotic dynamics of the system for exploration [44]. This method uses an RNN as an agent system and its internal chaotic dynamics as a source of exploration components. Shibata et al. hypothesize that the system can acquire transient dynamics with higher functions by developing its dynamics purposive through exploratory learning. Various studies have viewed brain activity as transitive or transient dynamics [45, 46, 47]. CBRL provides insights from a reinforcement learning perspective on studies of the exploratory nature and the transient dynamics of the brain. CBRL agents also have the advantage that their exploration can autonomously subside or resume depending on the situation. It has been suggested that CBRL agents can acquire higher exploration strategies that reflect their learned behavior [48]. CBRL offers a new perspective on both understanding the brain’s exploratory learning mechanisms and novel learning algorithms for AI.

The algorithms used in CBRL require treating deterministic and continuous action to eliminate stochastic exploration and human-designed action selection. Due to the necessity of a reinforcement learning algorithm that can handle deterministic and continuous actions without requiring random noise, Shibata et al. proposed causality trace learning and used it to train CBRL agents [44, 48, 49, 50]. However, this method has limited performance, and the CBRL algorithm is not yet well established. This study introduces the Twin Delayed Deep Deterministic Policy Gradient (TD3) algorithm, which is one of the state-of-the-art deep reinforcement learning algorithms designed for handling deterministic and continuous actions. The ability of the agent is evaluated by learning a simple goal task. We also examine how CBRL agents trained using TD3 respond to environmental changes. Furthermore, we investigate how the behavior of the agents changes depending on the levels of chaoticity in the model’s dynamics and how this affects their learning performance and ability to adapt to environmental changes.

This paper is organized as follows. Section 2 summarizes chaos-based reinforcement learning. Section 3 describes the experimental method. Section 4 presents the results of the experiments. Section 5 summarizes the conclusions of this study and discusses future research directions.

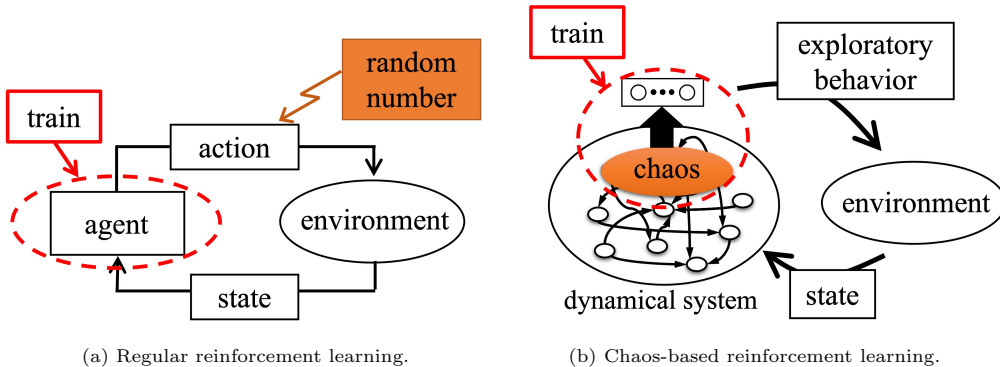


Fig. 1: Chaos-Based Reinforcement Learning (CBRL). (a) Overview of Regular Reinforcement Learning: The agent decides an action, and then stochastic choices or noise based on random numbers affect the action and drive exploration. The action changes the agent’s state through the environment. The agent improves its policy based on experience gained from the interactions. (b) Overview of CBRL: A dynamical system that exhibits chaotic behavior is used as the agent’s system. In CBRL, the agent behaves exploratively due to fluctuations caused by internal dynamics rather than external random numbers.

2. Chaos-based reinforcement learning

2.1. Exploration driven by internal chaotic dynamics

In the Chaos-based reinforcement learning method, the agent explores using internal chaotic dynamics. Figure 1 shows an overview of regular reinforcement learning and chaos-based reinforcement learning (CBRL). In general, exploration in reinforcement learning is performed probabilistically based on external random numbers. The ϵ -greedy method selects a random action with a probability of ϵ . The softmax policy selects an action stochastically using random numbers from a Boltzmann distribution of the state action values. Some algorithms for continuous action spaces explore by adding random noise to the action outputs for exploration purpose [51]. On the other hand, in CBRL, exploration is driven by chaotic dynamics within the agent system rather than relying on external random numbers.

A structure in which internal dynamics serves as the basis for exploration resources is plausible as a model of the biological brain and offers several learning benefits. As shown in Fig. 1(b), the source of exploration (i.e., chaotic dynamics) is a property of the agent system itself in CBRL. The properties of the system dynamics can be changed by learning. Therefore, the agent has the potential to optimize its exploration strategy through training. Previous studies have shown that CBRL agents can autonomously switch from an exploration mode to an exploitation mode as learning progresses [44, 52]. In the initial training episodes, when learning has not progressed sufficiently, the agent behaves chaotically and exploratively in the environment. As learning progresses, the system’s dynamics becomes more ordered, and the agent’s exploratory behavior subsides autonomously. Additionally, the agent can autonomously resume exploration when the environment changes its rules and the previously learned behavior is no longer rewarding.

2.2. Expectation for CBRL

Shibata et al. hypothesized that the key to creating systems with higher exploratory behavior and human-like intelligence is having a dynamical system with rich and spontaneous activity [44]. The dynamics of brain activity can be considered as a chaotic itinerancy [45] or as a process that transits through a series of saddle points [46]. The hypothesis expects the system to reconstruct its exploratory chaotic dynamics into transient dynamics that is purposeful to maximize rewards.

Since internal dynamics drives exploration, CBRL agents are also expected to be able to optimize exploration itself through learning. Goto et al. demonstrated that CBRL agents can change motor noise-like exploration into more sophisticated exploration that selects routes to avoid obstacles using an obstacle avoidance task [48, 49]. It is expected that CBRL agents can acquire more advanced exploration capabilities that effectively utilize previously acquired behaviors by constructing the agent’s internal state and decision-making processes as transitive dynamics such as chaotic itinerancy.

2.3. Issue of learning algorithm for CBRL

To ensure freedom and autonomy in learning, CBRL agents have used algorithms that deal with deterministic and continuous action spaces rather than stochastic and discrete ones in which action selections are defined heteronomously. In previous studies, the learning algorithm for CBRL agents has been an Actor-Critic, which can handle deterministic and continuous action spaces [44]. However, a classic Actor-Critic method that trains an actor using a correlation between the external exploration noise and the resulting change in value cannot be employed for CBRL, which does not use random number exploration. Therefore, causality trace learning, which is similar to Hebbian learning, has been proposed and employed as the training method for the actor-network [44, 48, 49, 50]. This method generates the teacher signal for the actor-network by multiplying the TD error by the input values stored in a tracing mechanism that changes the input tracing rate according to changes in the neuron’s output. However, this method has many problems, such as the inability to introduce the backpropagation method and the difficulty of learning complex tasks. Therefore, the learning algorithm for CBRL has not yet been sufficiently well-established.

3. Method

3.1. TD3

This study introduces Twin Delayed Deep Deterministic Policy Gradients (TD3) [53], a deep reinforcement learning algorithm that can handle deterministic policy and continuous action spaces, to CBRL. TD3 is an improved algorithm based on the model-free deep reinforcement learning method called “Deep Deterministic Policy Gradients” (DDPG) [51], and is one of the state-of-the-art reinforcement learning algorithms[53].

In the following part of this subsection, we first describe the DDPG and then the improvements introduced in TD3. In the DDPG, the agent model consists of an actor-network $\mu(s|\theta^\mu)$ and a critic network $Q(s, a|\theta^Q)$. Here, θ^μ and θ^Q are the weight value parameters of each network. $\mu(s|\theta^\mu)$ determines the action output a based on the agent’s state s and $Q(s, a|\theta^Q)$ estimates the state action value from s and a . Target networks

$\mu'(s|\theta^{\mu'})$ and $Q'(s, a|\theta^{Q'})$ are generated for each network with their weights copied and are used to generate the teacher signals to stabilize learning.

The agent acts in state s_t at each time t according to the following action output, to which the external exploration noise ϵ_t^a is added as follows:

$$a_t = \mu(s_t|\theta_t^\mu) + \epsilon_t^a. \quad (1)$$

As a result of the action, the agent receives the reward r_t , and the state transitions to $s'_t (= s_{t+1})$. The experience $e_t = (s_t, a_t, r_t, s'_t)$ is stored in the replay buffer \mathcal{B} .

Training is performed using N minibatch data of $e_i = (s_i, a_i, r_i, s'_i)$ randomly sampled from \mathcal{B} every step. Note that i indicates the index number of the samples in the N minibatch data. The teacher signal for the Critic network Q for the input data s_i and a_i is estimated as follows:

$$T_i^c = r_i + \gamma Q'(s'_i, \mu'(s'_i|\theta^{\mu'})|\theta^{Q'}), \quad (2)$$

where the discount rate $0 \leq \gamma \leq 1$ is a hyperparameter that determines the present value of future rewards. We then update θ^Q to minimize the loss function such that

$$L_Q = \frac{1}{N} \sum_i^N (T_i^c - Q(s_i, a_i|\theta^Q))^2. \quad (3)$$

The actor-network μ learns with deterministic policy gradient [54] estimated based on the sampled data:

$$\nabla_{\theta^\mu} J(\theta^\mu) \approx \frac{1}{N} \sum_i^N \nabla_{\mu(s_i)} Q(s_i, \mu(s_i|\theta^\mu)|\theta^Q) \nabla_{\theta^\mu} \mu(s_i|\theta^\mu), \quad (4)$$

where $J = \mathbb{E}[Q(s_i, \mu(s_i))]$. Note that θ^Q is fixed and only θ^μ is updated for training based on Equation (4). The target network weights $\theta^{Q'}$ and $\theta^{\mu'}$ are updated as follows:

$$\begin{aligned} \theta^{Q'} &\leftarrow \tau \theta^Q + (1 - \tau) \theta^{Q'}, \\ \theta^{\mu'} &\leftarrow \tau \theta^\mu + (1 - \tau) \theta^{\mu'}, \end{aligned} \quad (5)$$

where $0 < \tau \leq 1$ is the constant parameter that determines the update speed of the target network.

TD3 introduces three methods to the DDPG algorithm: Clipped Double Q-learning, Delayed Policy Updates, and Target Policy Smoothing. Clipped Double Q-learning is a method to suppress overestimation of the value by preparing two Critic networks Q_1 and Q_2 and adopting the smaller output value when generating teacher signals. Target Policy Smoothing is a technique to suppress the overfitting of Q to inaccurate value estimations by adding noise limited between $-C$ and C to the output of μ' during the generation of the teacher signal. With these techniques, the teacher signal for Q is given by

$$\begin{aligned} T_i^c &= r_i + \gamma \min_{j=1,2} Q'_j(s'_i, \mu'(s'_i|\theta^{\mu'}) + \epsilon_i^t|\theta^{Q'_j}), \\ \epsilon_i^t &\sim \text{clip}(\mathcal{N}(0, \sigma), -C, C). \end{aligned} \quad (7)$$

Note that the learning of μ by equation (4) always uses Q_1 . Therefore, the training is based on the following gradient

$$\nabla_{\theta^\mu} J(\theta^\mu) \approx \frac{1}{N} \sum_i^N \nabla_{\mu(s_i)} Q_1(s_i, \mu(s_i|\theta^\mu)|\theta^{Q_1}) \nabla_{\theta^\mu} \mu(s_i|\theta^\mu). \quad (8)$$

Delayed Policy Updates stabilizes learning by limiting updates of μ , μ' and Q' to once every d steps.

3.2. Reservoir network

CBRL requires the agent system to have chaotic dynamics. RNNs are dynamical systems and appropriate models for CBRL agents. However, training RNNs with CBRL presents a challenge in balancing the formation of convergent dynamics beneficial for completing the task while maintaining the chaotic dynamics required for exploration. To avoid this problem, we use a reservoir network (RN) that can be trained without modifying the parameters that determine the dynamical properties of the recurrent layer. Maass and Jaeger have proposed RNs as a Liquid State Machine (LSM) and an Echo State Network (ESN), respectively [55, 56]. In this study, we use an ESN composed of rate model neurons. The ESN consists of a recurrent layer called the “reservoir” and an output layer called the “readout.” The connection weights in the reservoir are randomly initialized and fixed, and only the weights from the reservoir to the readout are trained. The reservoir receives the time-series input and generates an output that nonlinearly reflects the spatio-temporal context of the input series. The readout generates the network output by performing a linear combination of the reservoir output and input. The dynamical properties of the ESN can be modified with a single fixed parameter. Therefore, it is easy to tune the chaoticity of the system during learning with chaos-based exploration [43]. Note that, in this study, the ESN is not used to process time series data but rather to generate chaotic dynamics in the agent system.

The structure of the ESN is shown in Fig. 2. The reservoir has N_x neurons that are recurrently connected with $\mathbf{W}^{\text{rec}} \in \mathbb{R}^{N_x \times N_x}$ with probability of p . The reservoir receives N_i -dimensional inputs through the weight matrix $\mathbf{W}^{\text{in}} \in \mathbb{R}^{N_x \times N_i}$. Then, the reservoir output is computed by the following equation:

$$\mathbf{x}_t = f(g\mathbf{W}^{\text{rec}}\mathbf{x}_{t-1} + \mathbf{W}^{\text{in}}\mathbf{u}_t), \quad (9)$$

where g is a scaling parameter that scales the strength of the recurrent connections and $\mathbf{u}_t \in \mathbb{R}^{N_i}$ is the input vector. $f(\cdot) = \tanh(\cdot)$ is the activation function applied element-wise. Typically, \mathbf{W}^{rec} is a sparse and fixed weight matrix initialized with a spectral radius of 1 by the following procedure. A random $N_x \times N_x$ matrix \mathbf{W} is generated (from a uniform distribution in this study), and then the elements of \mathbf{W} are set to 0 with probability of $(1-p)$. The matrix is normalized by its spectral radius ρ . Thus, the \mathbf{W}^{rec} is initialized as follows

$$\mathbf{W}^{\text{rec}} = \frac{1}{\rho} \mathbf{W}. \quad (10)$$

The arbitrary constant g can rescale the spectral radius of \mathbf{W}^{rec} . In general, g is usually set to $g < 1$ to fulfill the Echo State Property that requires the reservoir state to depend on past input series, but the influence of these inputs fades over finite time. A small g

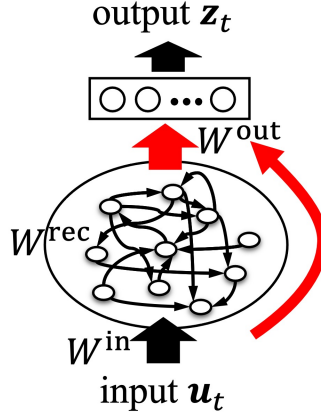


Fig. 2: Echo state network (ESN). An ESN has a reservoir that is a special recurrent layer whose recurrent and input weights are randomly and sparsely connected and fixed. Only the weights of the output layer (indicated by the red arrows) are trained.

tends to cause rapid decay of input context, while a large g tends to cause a slow decay of it. However, $g > 1$ sometimes achieves better performance, and it is argued that the best value for learning is realized when the reservoir dynamics is around the edge of chaos [57, 58]. When g is further increased beyond 1, and the reservoir dynamics crosses the edge of chaos, the reservoir state exhibits chaotic and spontaneous behavior. In this study, g is set larger than 1 to induce chaotic dynamics, which allows the CBRL agent to explore.

The network output $\mathbf{z}_t \in \mathbb{R}^{N_o}$ is calculated as

$$\mathbf{z}_t = \tanh(\mathbf{W}^{\text{out}}[\mathbf{x}_t; \mathbf{u}_t]), \quad (11)$$

where $\mathbf{W}^{\text{out}} \in \mathbb{R}^{N_o \times (N_x + N_i)}$ is the output weight matrix, N_o is the output dimension, and $[\cdot; \cdot]$ denotes the concatenation of two column vectors. \mathbf{W}^{out} is often fitted using algorithms such as ridge regression in reservoir computing. This study uses a reservoir network as an actor-network for CBRL agents. Since \mathbf{W}^{out} is trained by a slightly modified version of the TD3 algorithm as described in the following subsection, \mathbf{W}^{out} is updated by using gradient descent with the Adam optimizer [53].

3.3. TD3-CBRL

The following modifications are made to the TD3 algorithm to adapt to the CBRL approach. We eliminated the random number exploration noise ϵ^a and ϵ^t . Instead of exploration by random numbers, we rely on exploration driven spontaneously by chaotic dynamics and use an ESN with a larger spectral radius, as shown in Fig. 3(a), for the μ network. Here, $g = 2.2$ unless otherwise mentioned. We also add the reservoir output to the experience stored in the replay buffer. That is, $e_t = (\mathbf{u}_t, \mathbf{x}_t, a_t, r_t, \mathbf{u}_{t+1}, \mathbf{x}_{t+1})$ is stored into the replay buffer \mathcal{B} . The agent learns without the Back Propagation Through Time method using the stored \mathbf{u} and \mathbf{x} as state s_t . This method has been employed in several studies and efficiently trains deep reinforcement learning agents using ESN [59, 60]. TD3

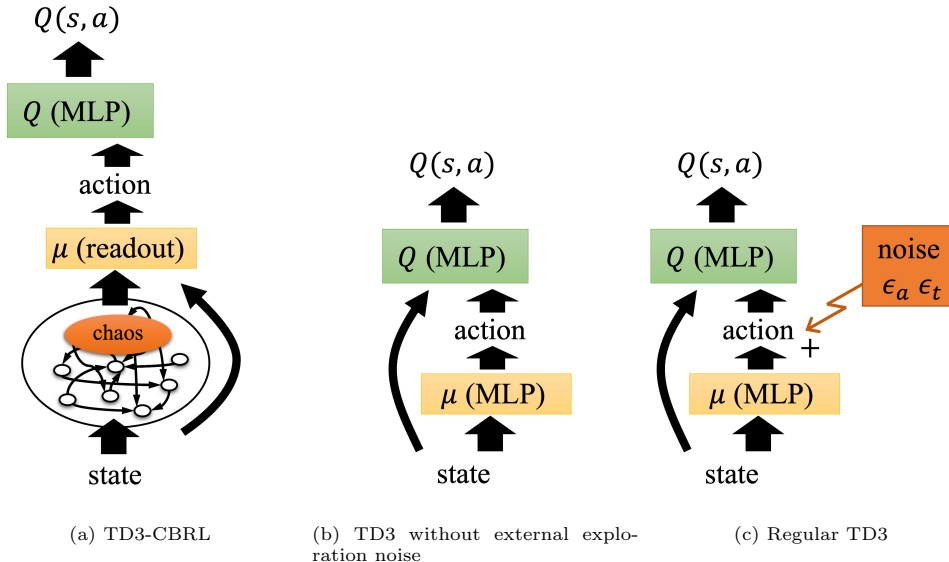


Fig. 3: Network Configurations. This study compares three network configurations of agents. (a) A TD3-CBRL agent, which uses a chaotic ESN in the actor-network μ . (b) An agent whose actor-network is an MLP with a hidden layer consisting of the same number of neurons as the reservoir in (a). In this case, the agent learns without the external random noises $\epsilon_a^t, \epsilon_t^t$ as added in the regular TD3. (c) An agent that has the same structure as (b) but trains using external random noise as in the regular TD3.

uses random numbers to randomly sample past experiences from the replay buffer. Since this sampling has an exploration-like effect with the random numbers, the replay buffer and batch sizes are set to the same value of 64 to eliminate this effect. Therefore, the training is based on the memory of the past 64 steps of experience. The variant of CBRL that introduces the above modified TD3 algorithm is called TD3-CBRL in this study. In the experiment, we compare the three cases shown in Fig. 3 (a-c) to confirm that the ESN dynamics contributes to the exploration during learning.

3.4. Goal task

This study uses a goal task to estimate the agent’s learning ability. Figure 4 shows the task outline. The task field is inside the range 0 to 20 on the x-y plane. There are 4 initial positions $(x, y) = (2, 2), (2, 18), (18, 2), (18, 18)$ in the environment. At the beginning of an episode, the agent is randomly placed at one of the initial positions, with Gaussian noise $\mathcal{N}(0, 1)$ added to its position in the field. The agent obtains an input \mathbf{u} based on its position (x^A, y^A) and uses it to determine its action outputs $-1 \leq a^x \leq 1$ and $-1 \leq a^y \leq 1$. As a result of the action, the agent’s position is updated according to the following equation

$$x_{t+1}^A = x_t^A + a_t^x, \quad (12)$$

$$y_{t+1}^A = y_t^A + a_t^y, \quad (13)$$

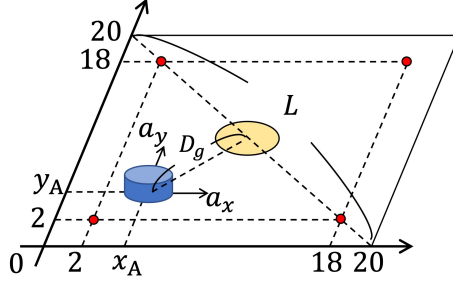


Fig. 4: Goal Task. The blue cylinder represents the agent, whose position is denoted by x^A and y^A . The field is surrounded by walls, and x^A and y^A cannot be out of the range from 0 to 20. The agent can move horizontally and vertically within the environment, with a maximum distance of 1 each. The yellow circle indicates the goal, and if the agent’s center is within this circle, the agent is rewarded and considered to have accomplished the task. The 4 red dots indicate the initial positions. At the beginning of each episode, the agent starts at one of these coordinates, with a slight noise added to the position.

where the agent cannot leave the task field and its range of movement is limited to $0 \leq x^A \leq 20$ and $0 \leq y^A \leq 20$. When the agent is at (x^A, y^A) , the input \mathbf{u} from the environment is given by

$$\mathbf{u} = \left[\frac{x^A}{20} \quad 1 - \frac{x^A}{20} \quad \frac{y^A}{20} \quad 1 - \frac{y^A}{20} \quad 1 - \frac{D_G}{2L} \right]^T, \quad (14)$$

where D_G is the Euclidean distance between the center of the agent and the goal, and L is the length of the diagonal of the task field. This task is episodic, and an episode ends when the agent either enters the goal circle of radius 2 (i.e., $D_G < 2$) or fails to reach the goal within 200 steps. The agent receives a reward of $r = 1$ for reaching the goal, $r = -0.01$ for colliding with the wall surrounding the field, and $r = 0$ for any other step.

We also examine a goal change task to estimate the ability to resume exploration and re-learn when the environment changes. This task initially places the goal at the initial position $G_p^1 = (15, 10)$, but changes the position to $G_p^2 = (5, 10)$ when the number of steps reaches N_c . After the goal change, the agent can no longer receive rewards for the behavior it has learned previously, and it needs to resume exploration and learn to reach the new goal to receive rewards again.

4. Experiment

4.1. Conditions

The reservoir size was set to $N_x = 256$ and the recurrent connection probability was set to $p = 0.1$. The input weight matrix W_{in} was sampled from a uniform distribution over $[-0.5, 0.5]$. The critic network is a fully connected Multilayer Perceptron (MLP) with two hidden layers consisting of 32 ReLU nodes, and the output neuron is a linear node. The initial weights were set using the default settings in PyTorch (version 1.13.1 in this study.). Both the critic Q and the actor μ are trained using the Adam optimizer, with a learning rate of 0.0003. We paused training every N_v steps and verified the

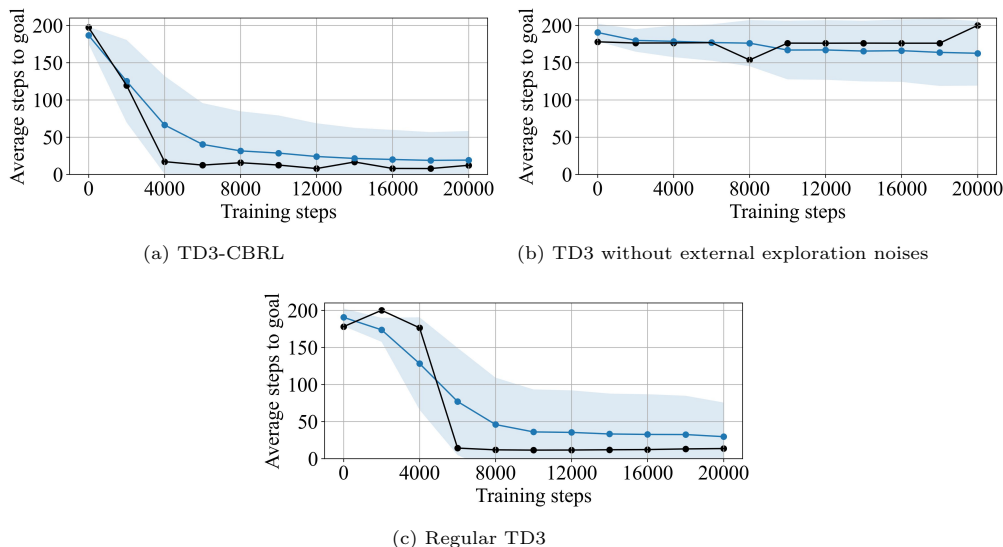


Fig. 5: Learning curves. The vertical axis shows the average number of steps required to reach the goal starting from the 16 initial positions. The horizontal axis shows the training steps. The black line shows the representative results with a specific random seed, and the blue line and shaded area show the mean and standard deviation of the steps from the results of experiments with 100 different random number seeds. (a) shows the learning results with TD3-CBRL. (b) shows the learning results with TD3 without external exploration noises. (c) shows the learning results with regular TD3.

agent’s behavior starting from 8 initial positions $(2, 2)$, $(2, 10)$, $(2, 18)$, $(10, 2)$, $(10, 18)$, $(18, 2)$, $(18, 10)$, $(18, 18)$ and slightly different positions (shifted 0.002 in the x and y axes, respectively). The replay buffer size and batch size were both set to 64. The discount rate γ was set to 0.95. The time constant τ of the target network was set to 0.05. We set $\epsilon^a = 0$, $\epsilon^t = 0$, and the Delayed Policy Updates step to $d = 2$.

4.2. Learning result

The TD3-CBRL agent learned the goal task in 20000 steps. Figure 5(a) shows the learning curve resulting from the test conducted every $N_v = 2000$ step. This figure shows that the average number of steps required by the agent to reach the goal decreases as the learning progresses. This result indicates that TD3-CBRL can successfully learn the goal task. Figure 6(a) shows the trajectories of the agent’s movement in the environment for each test trial. This figure shows that in the initial stage of learning (0 step), the agent acts exploratively in the environment. On the other hand, in the trajectories after 4000 steps, the agent is moving toward the goal from each initial position, although it takes detours in some cases. We also see that the exploratory behavior subsides as the learning progresses. It is important to note that no external random noises for exploration were added to the agent’s action output during the learning process. This result indicates that the internal dynamics of the reservoir caused spontaneous exploratory behavior, and as learning progressed, such variability in the output was autonomously suppressed.

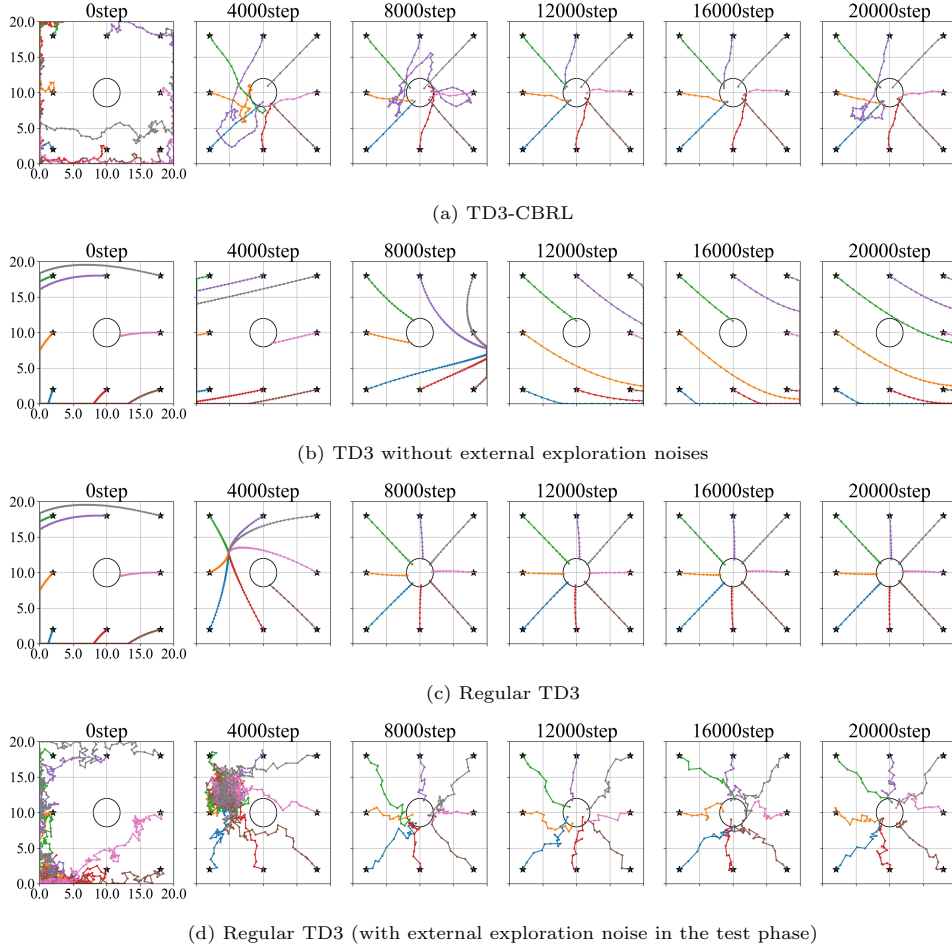


Fig. 6: Agent trajectories during the test. Each colored trajectory represents the agent’s behavior from the 8 initial test positions. Each graph in the subfigures shows the test results at 0, 4000, 8000, 12000, 16000, and 20000 training steps. The random seed is the same as the one used for the representative results in Fig. 5. (a) shows the training results for TD3-CBRL. (b) shows the results of TD3 without exploration by random noises. (c) shows the results with regular TD3. (d) shows the behavior of the same agent as in (c) when the exploration by random noises is not stopped during the test.

As seen in the purple trajectory where the agent starts from the initial position (10,18) in Fig. 6(a), the agent wandered to the left around the goal before reaching it at the 20000 step, even though the agent had already learned to reach the goal in a straight path by the 12000 step. This result seems to be caused by the chaoticity of the agent’s dynamics, which causes its behavior to change sensitively depending on the initial position and parameter changes. Figure 7 (a) shows the results of investigating the sensitivity of the agent’s behavior to variations of the initial positions in this case. This figure shows the trajectories of agents starting from slightly different initial positions. At the 0 step, the agent, starting from its original initial position, continues toward the wall and ends the episode without reaching the goal. On the other hand, although the

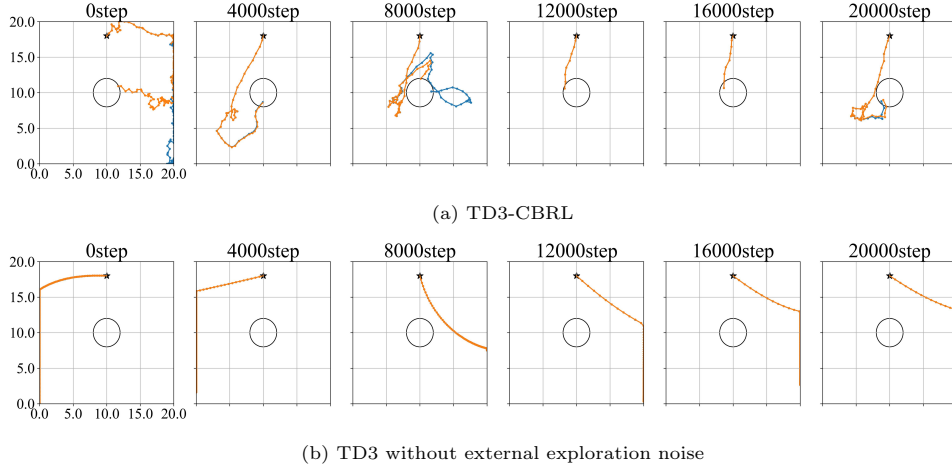
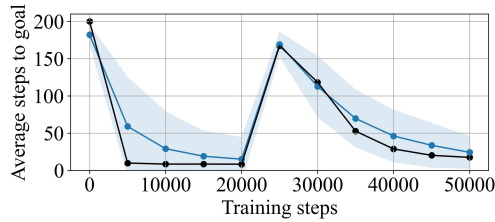


Fig. 7: Sensitivity of agent trajectories for initial position. The blue and orange lines show the agent’s trajectory when the agent started from (10, 18) and from a slightly shifted initial position (10.002, 18.002), respectively. Each graph in the subfigure shows the test results at 0, 4000, 8000, 12000, 16000, and 20000 training steps.

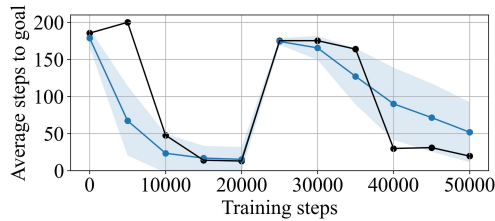
agent starting from the slightly shifted position behaves like the agent starting from the original initial position initially, it leaves the original trajectory after a while and eventually reaches the goal. This result indicates that in the early phases of learning, a slight difference in the initial position can significantly change the agent’s behavior and even determine the task’s success or failure. At the 8000 step, the two agents eventually reach the goal, but their paths diverge from the middle of the episode. The agent, starting from the original initial position, explores both the left and right sides before reaching the goal. On the other hand, the agent starting from a slightly different point did not explore the right side of the goal; instead, it went to the goal. Thus, the sensitivity to the initial condition of the TD3-CBRL agent allows it to exhibit both exploration driven by the chaoticity and exploitation of its previously learned behavior.

4.3. Effects by presence or absence of exploration component

To confirm that the chaoticity of the model contributes to the agent’s exploration, we evaluated the learning performance when the model does not have chaotic dynamics. Specifically, instead of an actor-network with a chaotic reservoir, we used a Multilayer Perceptron (MLP) with one hidden layer consisting of 256 tanh neurons, as shown in Fig. 3 (b). In this case, the learning rate was readjusted to 0.00003. Figure 5(b) shows the learning curve for the MLP case without exploration random noise. This figure shows that the number of steps to the goal did not decrease and that the agent failed to learn the goal task. Figure 6(b) and Fig. 7 (b) show the agent trajectory during the test phase and the sensitivity test under this condition. These figures show that the agent lacked exploratory behavior and failed to learn. This result appears to be due to the fact that the learning model did not have the dynamics to generate spontaneous activity, and thus, the exploration did not occur without random noises.



(a) Regular case ($g = 2.2$).



(b) Larger spectral radius case ($g = 5$).

Fig. 8: Learning curves of goal change task. The definitions of line colors are the same as in Fig. 5.

To clarify that the absence of exploration random noise is the direct cause of the learning failure, we verified the case where the MLP is trained with random noise for exploration in the same way as in the regular TD3, as shown in Fig. 3 (c). Figure 5(c) shows the learning curve under this condition. This figure shows that the number of steps to reach the goal decreased and that the agent succeeded in learning the task. Figure 6(c) shows the trajectories of the agent’s behavior in this validation. This figure shows that the agent can learn the behavior of moving toward the goal due to exploration with random numbers during the learning process. Note that during the test phase, adding random numbers to the action outputs is stopped. These results indicate that the presence or absence of exploration by random numbers has a significant influence on the success or failure of learning and that the TD3-CBRL agent successfully learns the goal task through exploration driven by the chaotic dynamics of the reservoir.

Comparing (a) and (c) in Fig. 6, the regular TD3 agent can go to the goal in a straighter path than the TD3-CBRL agent. However, this is due to an external intervention that removes the random noise during the test phase. Figure 6(d) shows the result when the agent in (c) acts with the exploration random noise during the test phase. If the exploration random noise is not eliminated, the agent cannot reach the goal in a straight path. On the other hand, the TD3-CBRL agent can autonomously reduce the variability driven by its chaoticity as its learning progresses, although there are still cases where it takes detours depending on its initial position. This is a beneficial property and a limitation of the CBRL agent.

4.4. Goal change task.

Previous studies have shown that when the environment changes and the agent cannot be rewarded with previously learned behaviors, CBRL agents can autonomously resume their exploration and learn to adapt to the new environment [44]. These results suggest that CBRL agents have the flexibility to adapt to dynamic and uncertain environments.

Here, we observed the agent’s response to changing the goal position to test whether TD3-CBRL agents can re-learn when the task rule changes.

In the goal change task, the goal was initially placed at $G_p^1 = (15, 10)$, and learning was performed for 20000 steps. Then, at the $N_c = 20001$ step, the goal position was changed to $G_p^2 = (5, 10)$, and learning continued in the new environment for another 30000 steps. The test is conducted every $N_v = 2000$ step. The learning curve under these conditions is shown in Fig. 8(a). This figure shows that when the goal position is changed, the number of steps required to reach the goal, which had decreased during learning in the initial environment, temporarily increases. However, as learning in the new environment progresses, the number of steps decreases again. This result indicates that the agent is adapting to the new environment.

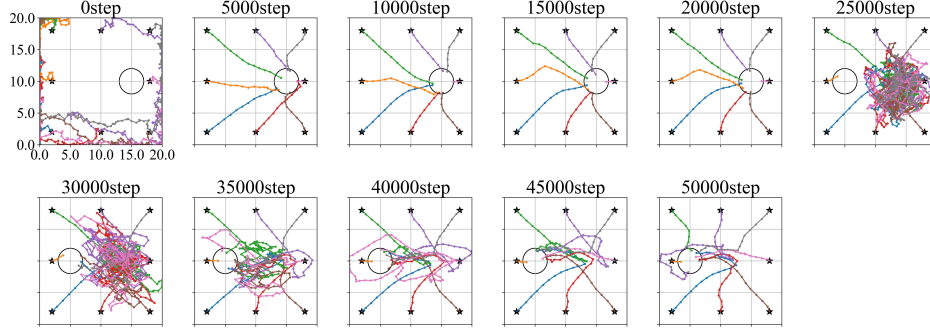
The trajectories of the agent in the environment under these conditions are shown in Fig. 9(a). This figure shows that at the 25000 steps, the agent autonomously resumes its exploration with internal chaotic dynamics due to the change in the goal position. After that, the agent gradually adapts its behavior to move toward the new goal.

4.5. Learning performance and chaoticity

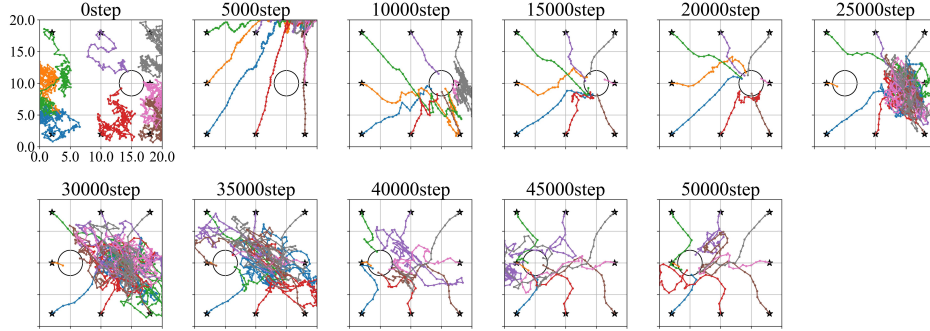
We investigated the effect of the chaoticity of the system on learning performance. The chaoticity of the reservoir network can be tuned by changing the spectral radius of the reservoir’s recurrent weight matrix using the parameter g . We changed the value of g from 0 to 12 in 0.2 increments and conducted trials with 100 different random number seeds under each condition to obtain the learning success probability and the average number of steps to reach the goal. Here, success is defined as an event when the agent reaches the goal from all 16 initial positions during the final test. The results are shown in Fig. 10(a). This figure shows that learning performance begins to improve as g exceeds around 1, and learning becomes successful in most cases when g exceeds approximately 2. This result indicates that the chaoticity of the system is essential for successful exploration and learning. The results also indicate that the probability of success remains high even when the value of g is further increased. In general, there is an appropriate range for the parameter g for time series processing in reservoir computing. It can be considered that since this study does not target tasks that require memory and the task is simple, the success probability of learning by TD3-CBRL remains stable even when g is larger than the typical critical value.

We examined how the flexibility of switching between exploration and exploitation was affected by the value of g . The value of g was changed from 0 to 12 in 0.2 increments, and a goal change task was learned under 100 different random number seeds to ensure statistical validity. The task settings are the same as in Section 4.4 except for g . The results are shown in Fig. 10(b). This figure shows that performance on the goal change task decreases with an extremely large g . This result suggests that when g is extremely large, the balance between exploration and exploitation is lost, and the flexibility to deal with environmental changes is reduced. These results indicate that choosing an appropriate g value is still essential in CBRL using reservoir networks.

We experimented with long-term re-learning to investigate whether a larger g decreases the model’s re-learning ability or increases the number of steps required for re-learning. Specifically, after changing the goal position at the $N_c = 20001$ step, the agent learned for 180000 steps in the new environment. The results are shown in Fig. 10(c). This figure shows that long-term learning mitigated the decrease in learning performance



(a) Regular case ($g = 2.2$)



(b) Larger spectral radius case ($g = 5$)

Fig. 9: Agent trajectories during the test of the goal change task. Each graph in the subfigures shows the test results conducted every 5000 training steps. The definitions of the line colors are the same as in Fig. 6.

when g is large. This result indicates that a model with a larger g and stronger chaoticity requires more re-learning steps, consequently making re-learning more difficult.

4.6. Readout weights and chaoticity

To clarify the reason for the increase in steps required for re-learning when g is extremely large, we investigated how the acquired readout weights vary with the spectral radius g , which adjusts the chaoticity of the reservoir. The inputs for the readout are the reservoir output and the agent's state in the environment. They are received through 256 and 5 weights, respectively. Figure 11 shows the readout weights after training for spectral radius g of 2.2 and 5. The blue dots show the weights from the reservoir, and the red dots show the bypass weights. Comparing these figures, we can see that the bypass weights are larger for the case of $g = 5$ than for the case of $g = 2.2$, and the weights from the reservoir are relatively smaller than the bypass weights. Figure 12 shows how the average of the absolute values of the weights from the reservoir and the

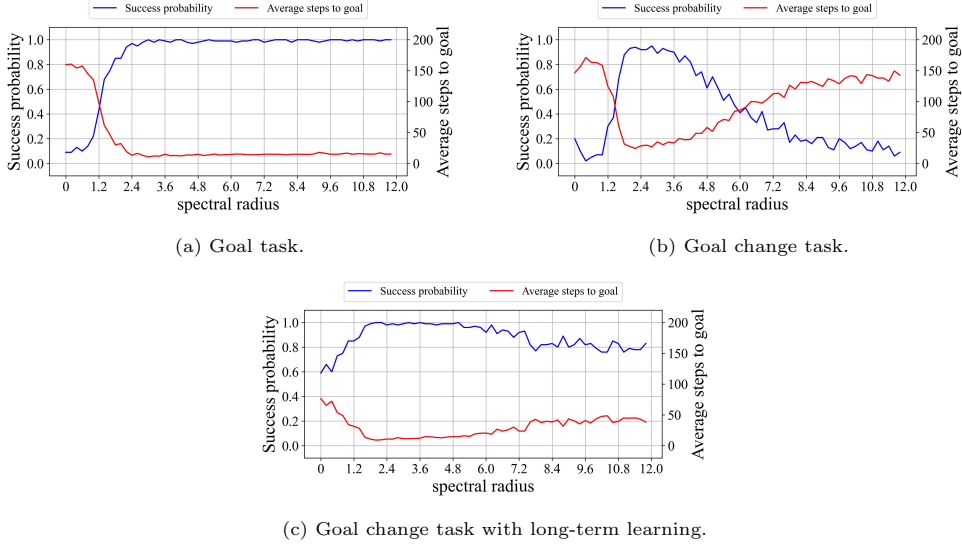


Fig. 10: Learning performance with varying spectral radius. The blue line shows the learning success probability, indicated on the left vertical axis. The red line shows the average number of steps required to reach the goal, indicated on the right vertical axis. The horizontal axis shows the value of the spectral radius. (a) shows the learning results for the goal task. (b) shows the learning results of the goal change task. (c) shows the results of learning over a long period of 18,000 steps after the goal change.

bypass weights change when the spectral radius is varied. This figure shows that the bypass weights increase as the spectral radius increases. This result suggests that the agent ignores the reservoir outputs and focuses more on the state inputs directly given from the environment.

We have validated the goal change task with $g = 5$. Figure 8(b) shows the results of this validation. Comparing this with the result under the setting of $g = 2.2$ shown in Fig. 8(a), re-learning convergence was slower when $g = 5$. Figure 9(b) shows the agent’s behavior in the environment at $g = 5$. Comparing Fig. 9(a) and (b), we can see that in the case of $g = 5$, the agent continues its exploratory behavior for more steps and takes more steps to shift to an exploitation mode. This slow re-learning seems to be because more updates are required to modify the larger bypass weights to adapt them to the new environment when the spectral radius is large. To clarify this, we analyzed the change in the bypass weights in the re-learning task, and Fig. 13 shows the results. Comparing the two results, the bypass weight change in the case of $g = 5$ is significantly larger than in the case of $g = 2.2$. In the case of $g = 5$, the bypass weights increased to attend to state inputs, ignoring the reservoir’s chaoticity, and thus, more steps are required. These results confirm that the inflated bypass weights inhibit flexible switching between exploration and exploitation. These results indicate that an excessive spectral radius and agent chaoticity impair the ability of TD3-CBRL agents to properly balance exploration and exploitation properly.

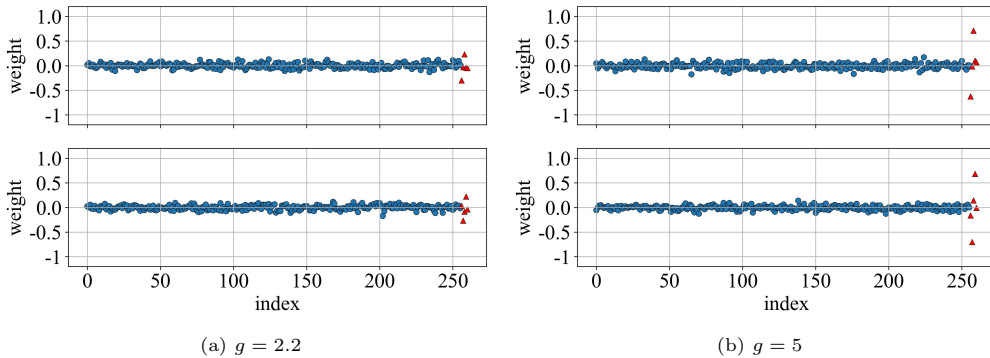


Fig. 11: Readout weights. Blue dots indicate 256 weights from the reservoir to the readout. The red triangles show the bypass weights through which the state of the environment is given directly to the readout. (a) shows the result when $g = 2.2$. (b) shows the result when $g = 5$. The upper and lower figures show the weights given to the action output decision unit in the x -axis and y -axis directions, respectively.

4.7. Exploration with random number layer

The above verification confirmed that learning proceeds to ignore the reservoir’s output if the reservoir is too chaotic. To verify this result further, we investigated learning when a random vector of independent and identically distributed random numbers replaces the reservoir. Specifically, we replaced the reservoir with a uniform random vector sampled from $[-1, 1]$ and conducted learning under this condition. In this setting, the random vector serves as the exploration component but is worthless as information about the agent’s state. Figure 14 shows the results of this experiment. This figure shows that the agent succeeded in learning the task even when a random number vector replaces the reservoir, although the number of steps required for learning tends to increase. The learning results for the readout weights under this situation show that the bypass weights are significantly larger than the weights from the random layer. This result seems to be because the random layer’s output is worthless for accomplishing the task and suggests that a similar phenomenon occurs when the spectral radius of the reservoir is too high.

We experimented with a goal change task to verify whether the exploration with a random layer is flexible enough to adapt to environmental changes. The task settings are the same as in Section 4.4. Figure 15 shows the experimental results under these conditions. This figure shows that the random layer model failed to learn the goal change task. This result indicates that the model with the random layer cannot flexibly switch between exploration and exploitation.

5. Conclusion

This study introduced TD3 as a learning algorithm for chaos-based reinforcement learning (CBRL) and revealed several characteristics.

It was confirmed that the TD3-CBRL agent can learn the goal task. This suggests that TD3 is a good candidate as a learning algorithm for CBRL, which had not been well-established in previous studies. Although a regular TD3 agent succeeded in learning the goal task, the agent failed to learn it without external exploration noise, despite the simplicity of the task. On the other hand, the TD3-CBRL agent, whose actor model has

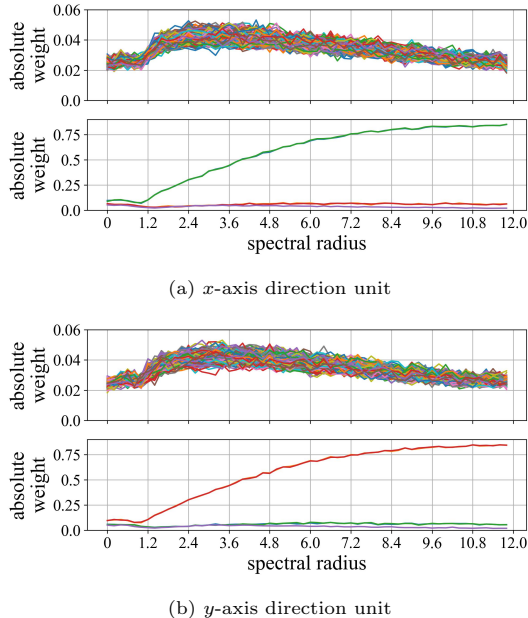


Fig. 12: Spectral radius and readout weights. The vertical axis shows the absolute average of the learned weights across 100 different random seeds. The horizontal axis shows the spectral radius. The upper graph shows the 256 weights from the reservoir to the readout, and the lower graph shows the 5 bypass weights. (a) and (b) show the weights of the readout units that determine the travel distance a^x , a^y in the x and y axes, respectively.

chaotic dynamics, can learn without exploration with random noises. This comparison indicates that the internal chaotic dynamics of the reservoir contributes to the agent’s exploratory behavior.

We also observed the agent’s adaptation to the environmental change of altering the goal position during the learning process and found that the agent resumed chaotic exploration and successfully re-learned. Furthermore, our results indicate that there is an appropriate range for the strength of internal chaos for the TD3-CBRL agent to have the flexibility to autonomously switch between exploration and exploitation modes. In particular, it was found that when the spectral radius is too large, the weights from the bypass become excessively large. Then, the inflated weights negatively affect the flexibility of switching between exploration and exploitation. These results indicate that the appropriate choice of spectral radius is essential in designing reservoir networks in CBRL to achieve a proper balance between exploration and exploitation.

We tested the TD3-CBRL agent when the reservoir network, the source of the exploration dynamics, was replaced by a random vector. The results showed that the agent could learn the goal task, but the bypass weights became significantly large, and the agent failed to learn the goal change task. These results indicate that the reservoir, which generates the dynamics in CBRL, does not act just as a mere noise source. While the random vectors do not reflect any external input, the reservoir creates a variety of background activities in the system incorporating the input’s influence. This activity

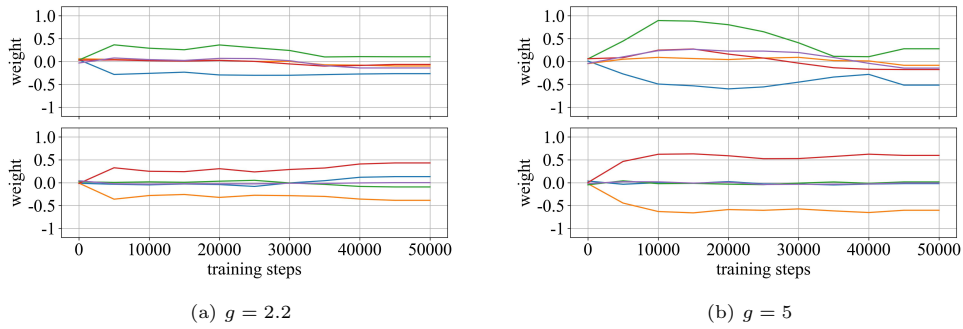


Fig. 13: Changes in the weights of the bypass. The vertical axis shows the weights, and the horizontal axis shows the number of training steps. (a) and (b) show the results at $g = 2.2$ and $g = 5$, respectively. The upper and lower figures show the weights of the readout unit in the x -axis and y -axis directions, respectively.

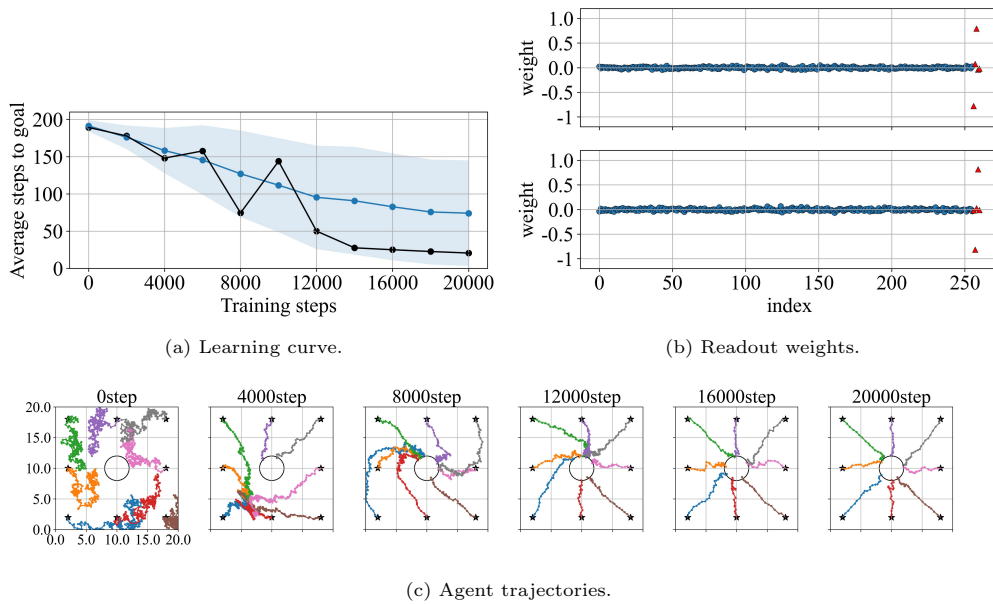


Fig. 14: Result when a random vector is used instead of a reservoir. The definitions of line colors are the same as in Fig. 5, 6, and 11.

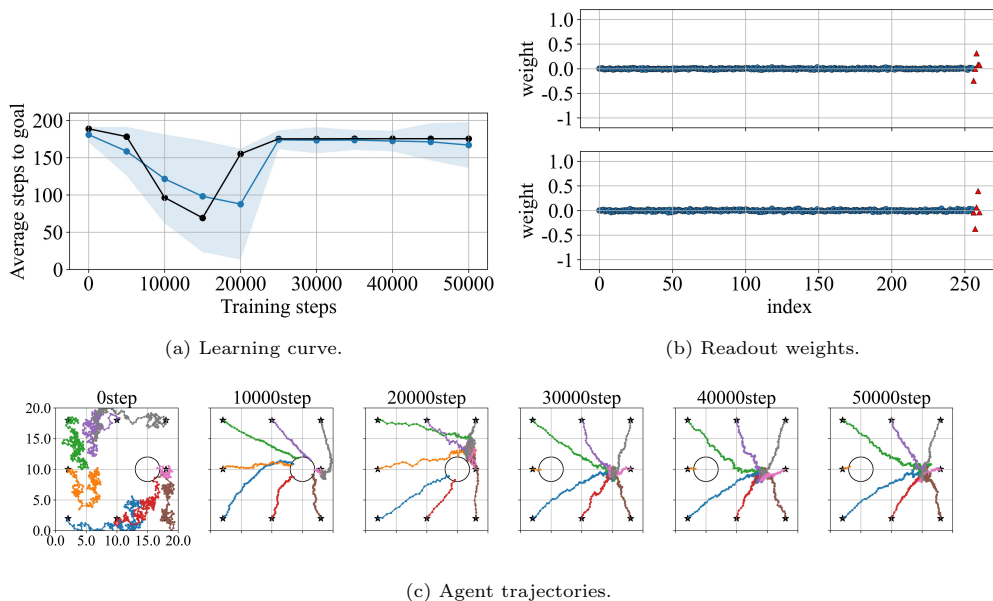


Fig. 15: Result of the goal change task when a random vector is used instead of a reservoir. The definitions of the line colors are the same as in Fig. 5, 6, and 11.

seems to provide the variability necessary for exploration and to be a resource that drives new exploratory behavior when encountering unknown experiences.

Various studies have shown that neural populations operate in a critical state [61, 62, 63, 64]. Reservoir network performance has also been shown to be optimized at the edges of chaos [57, 58]. In addition, a study in which ESNs performed chaos-based exploration learning also showed results suggesting that exploration and exploitation are balanced at the edges of chaos [43]. In this study, the spectral radius was not optimal around $g = 1$, where the reservoir dynamics is typically on the edge of chaos. One hypothesis for explaining this result is that the spectral radius of the subsystem, the reservoir, needed to be larger to place the entire system’s dynamics, including the environment, at the edge of chaos. It is important to verify this by focusing on the entire system’s behavior, including the interaction between the CBRL agent and the environment.

This study introduced TD3 to CBRL and validated its ability with a simple task to investigate learning and re-learning in detail. In previous studies and this one, CBRL has yet to learn difficult benchmark tasks used for deep reinforcement learning research, such as Atari game tasks and nonlinear control tasks using MUJOCO. In future works, improving the model to learn more difficult tasks is necessary. A wider selection of tasks will allow us to examine CBRL from newer perspectives.

Introducing the new reservoir structure proposed to extend its performance is useful to improve the learning performance of CBRL. Reservoirs do not perform well with high-dimensional input such as images. Several studies have proposed methods that use untrained CNNs for feature extraction [65, 66]. Introducing these methods can enable CBRL agents to learn tasks with high-dimensional input, such as raw images. Structural improvement that constructs reservoirs in multiple layers [67, 68, 69] and methods that reduce the model size by using multi-step reservoir outputs as input to readouts [70] have

been proposed. It is worth verifying the use of these new reservoir techniques to improve the performance of CBRL agents.

Improvements in learning algorithms are also worth considering. Sensitivity adjustment learning (SAL), which adjusts the chaoticity of neurons based on "sensitivity," has been proposed [71]. This method can modify the recurrent weights while keeping the chaoticity of the RNN. Using SAL to maintain chaoticity and learning with Backpropagation Through Time may allow CBRL agents to learn more difficult tasks. Self-modulated reservoir computing (SM-RC) that extends the reservoir network's ability by dynamically changing the characteristics of the reservoir and attention to the input through a self-modulated function has been proposed [72]. Since SM-RC can adjust its spectral radius, it is also expected that CBRL agents with SM-RC can learn to change their chaoticity and switch between exploration and exploitation states more dynamically.

Acknowledgments

The author would like to thank Prof. Katsunari Shibata for useful discussions about this research. This work was supported by Moonshot R&D Grant Number JPMJMS2021, AMED under Grant Number JP23dm0307009, Institute of AI and Beyond of UTokyo, the International Research Center for Neurointelligence (WPI-IRCIN) at The University of Tokyo Institutes for Advanced Study (UTIAS), JSPS KAKENHI Grant Numbers JP20H05921, JP22K17969, JP22KK0159.

References

- [1] D. Hassabis, D. Kumaran, C. Summerfield, M. Botvinick, Neuroscience-inspired artificial intelligence, *Neuron* 95 (2) (2017) 245–258.
- [2] A. Krizhevsky, I. Sutskever, G. E. Hinton, Imagenet classification with deep convolutional neural networks, in: *Advances in neural information processing systems*, 2012, pp. 1097–1105.
- [3] K. Simonyan, A. Zisserman, Very deep convolutional networks for large-scale image recognition, arXiv preprint arXiv:1409.1556.
- [4] K. He, X. Zhang, S. Ren, J. Sun, Deep residual learning for image recognition, in: *Proceedings of the IEEE conference on computer vision and pattern recognition*, 2016, pp. 770–778.
- [5] A. Graves, N. Jaitly, Towards end-to-end speech recognition with recurrent neural networks, in: *International conference on machine learning*, 2014, pp. 1764–1772.
- [6] D. Amodei, S. Ananthanarayanan, R. Anubhai, J. Bai, E. Battenberg, C. Case, J. Casper, B. Catanzaro, Q. Cheng, G. Chen, et al., Deep speech 2: End-to-end speech recognition in english and mandarin, in: *International conference on machine learning*, 2016, pp. 173–182.
- [7] K. Cho, B. Van Merriënboer, C. Gulcehre, D. Bahdanau, F. Bougares, H. Schwenk, Y. Bengio, Learning phrase representations using rnn encoder-decoder for statistical machine translation, arXiv preprint arXiv:1406.1078.
- [8] I. Sutskever, O. Vinyals, Q. V. Le, Sequence to sequence learning with neural networks, *Advances in neural information processing systems* 27.
- [9] A. Vaswani, N. Shazeer, N. Parmar, J. Uszkoreit, L. Jones, A. N. Gomez, L. Kaiser, I. Polosukhin, Attention is all you need, *Advances in neural information processing systems* 30.
- [10] J. Devlin, M.-W. Chang, K. Lee, K. Toutanova, Bert: Pre-training of deep bidirectional transformers for language understanding, arXiv preprint arXiv:1810.04805.
- [11] A. Dosovitskiy, L. Beyer, A. Kolesnikov, D. Weissenborn, X. Zhai, T. Unterthiner, M. Dehghani, M. Minderer, G. Heigold, S. Gelly, et al., An image is worth 16x16 words: Transformers for image recognition at scale, arXiv preprint arXiv:2010.11929.
- [12] A. Radford, J. W. Kim, T. Xu, G. Brockman, C. McLeavey, I. Sutskever, Robust speech recognition via large-scale weak supervision, in: *International Conference on Machine Learning*, PMLR, 2023, pp. 28492–28518.

- [13] T. Brooks, B. Peebles, C. Homes, W. DePue, Y. Guo, L. Jing, D. Schnurr, J. Taylor, T. Luhman, E. Luhman, C. W. Y. Ng, R. Wang, A. Ramesh, Video generation models as world simulators. URL <https://openai.com/research/video-generation-models-as-world-simulators>
- [14] G. Franceschelli, M. Musolesi, On the creativity of large language models, arXiv preprint arXiv:2304.00008.
- [15] E. E. Guzik, C. Byrge, C. Gilde, The originality of machines: Ai takes the torrance test, *Journal of Creativity* 33 (3) (2023) 100065.
- [16] W. X. Zhao, K. Zhou, J. Li, T. Tang, X. Wang, Y. Hou, Y. Min, B. Zhang, J. Zhang, Z. Dong, et al., A survey of large language models, arXiv preprint arXiv:2303.18223.
- [17] J. McCarthy, M. L. Minsky, N. Rochester, C. E. Shannon, A proposal for the dartmouth summer research project on artificial intelligence.
- [18] R. S. Sutton, A. G. Barto, Reinforcement learning: An introduction, MIT press, 2018.
- [19] C. W. Anderson, Strategy learning with multilayer connectionist representations, in: *Proceedings of the Fourth International Workshop on Machine Learning*, Elsevier, 1987, pp. 103–114.
- [20] C. W. Anderson, Learning to control an inverted pendulum using neural networks, *IEEE Control Systems Magazine* 9 (3) (1989) 31–37.
- [21] L.-J. Lin, Reinforcement learning for robots using neural networks, Carnegie Mellon University, 1992.
- [22] G. Tesauro, Temporal difference learning and td-gammon, *Communications of the ACM* 38 (3) (1995) 58–68.
- [23] K. Shibata, T. Kawano, Learning of action generation from raw camera images in a real-world-like environment by simple coupling of reinforcement learning and a neural network, in: *International Conference on Neural Information Processing*, Springer, 2008, pp. 755–762.
- [24] V. Mnih, K. Kavukcuoglu, D. Silver, A. Graves, I. Antonoglou, D. Wierstra, M. Riedmiller, Playing atari with deep reinforcement learning, arXiv preprint arXiv:1312.5602.
- [25] H. Van Hasselt, A. Guez, D. Silver, Deep reinforcement learning with double q-learning, in: *Proceedings of the AAAI conference on artificial intelligence*, Vol. 30, 2016.
- [26] Z. Wang, T. Schaul, M. Hessel, H. Hasselt, M. Lanctot, N. Freitas, Dueling network architectures for deep reinforcement learning, in: *International conference on machine learning*, PMLR, 2016, pp. 1995–2003.
- [27] D. Horgan, J. Quan, D. Budden, G. Barth-Maron, M. Hessel, H. Van Hasselt, D. Silver, Distributed prioritized experience replay, arXiv preprint arXiv:1803.00933.
- [28] S. Kapturowski, G. Ostrovski, J. Quan, R. Munos, W. Dabney, Recurrent experience replay in distributed reinforcement learning, in: *International conference on learning representations*, 2018.
- [29] D. Silver, J. Schrittwieser, K. Simonyan, I. Antonoglou, A. Huang, A. Guez, T. Hubert, L. Baker, M. Lai, A. Bolton, et al., Mastering the game of go without human knowledge, *nature* 550 (7676) (2017) 354–359.
- [30] D. Silver, T. Hubert, J. Schrittwieser, I. Antonoglou, M. Lai, A. Guez, M. Lanctot, L. Sifre, D. Kumaran, T. Graepel, et al., A general reinforcement learning algorithm that masters chess, shogi, and go through self-play, *Science* 362 (6419) (2018) 1140–1144.
- [31] A. P. Badia, B. Piot, S. Kapturowski, P. Sprechmann, A. Vitvitskyi, Z. D. Guo, C. Blundell, Agent57: Outperforming the atari human benchmark, in: *International conference on machine learning*, PMLR, 2020, pp. 507–517.
- [32] A. Fontanini, D. B. Katz, Behavioral states, network states, and sensory response variability, *Journal of Neurophysiology* 100 (3) (2008) 1160–1168.
- [33] K. L. Briggman, H. D. Abarbanel, W. Kristan Jr, Optical imaging of neuronal populations during decision-making, *Science* 307 (5711) (2005) 896–901.
- [34] M. D. Fox, A. Z. Snyder, J. L. Vincent, M. E. Raichle, Intrinsic fluctuations within cortical systems account for intertrial variability in human behavior, *Neuron* 56 (1) (2007) 171–184.
- [35] W. J. Freeman, The physiology of perception, *Scientific American* 264 (2) (1991) 78–87.
- [36] C. A. Skarda, W. J. Freeman, How brains make chaos in order to make sense of the world, *Behavioral and brain sciences* 10 (2) (1987) 161–173.
- [37] K. Aihara, T. Numajiri, G. Matsumoto, M. Kotani, Structures of attractors in periodically forced neural oscillators, *Physics Letters A* 116 (7) (1986) 313–317.
- [38] K. Aihara, T. Takabe, M. Toyoda, Chaotic neural networks, *Physics letters A* 144 (6-7) (1990) 333–340.
- [39] M. Adachi, K. Aihara, Associative dynamics in a chaotic neural network, *Neural Networks* 10 (1) (1997) 83–98.
- [40] L. Chen, K. Aihara, Chaotic simulated annealing by a neural network model with transient chaos,

- Neural networks 8 (6) (1995) 915–930.
- [41] M. Hoerzer, Gregor, R. Legenstein, W. Maass, Emergence of complex computational structures from chaotic neural networks through reward-modulated hebbian learning, *Cerebral cortex* 24 (3) (2012) 677–690.
 - [42] T. Matsuki, K. Shibata, Reward-based learning of a memory-required task based on the internal dynamics of a chaotic neural network, in: *International Conference on Neural Information Processing*, Springer, 2016, pp. 376–383.
 - [43] T. Matsuki, K. Shibata, Adaptive balancing of exploration and exploitation around the edge of chaos in internal-chaos-based learning, *Neural Networks* 132 (2020) 19–29.
 - [44] K. Shibata, Y. Sakashita, Reinforcement learning with internal-dynamics-based exploration using a chaotic neural network, in: *2015 International Joint Conference on Neural Networks (IJCNN)*, 2015, pp. 1–8.
 - [45] K. Kaneko, I. Tsuda, Chaotic itinerancy, *Chaos: An Interdisciplinary Journal of Nonlinear Science* 13 (3) (2003) 926–936.
 - [46] M. I. Rabinovich, R. Huerta, P. Varona, V. S. Afraimovich, Transient cognitive dynamics, metastability, and decision making, *PLoS computational biology* 4 (5) (2008) e1000072.
 - [47] T. Kanamaru, T. K. Hensch, K. Aihara, Maximal memory capacity near the edge of chaos in balanced cortical ei networks, *Neural Computation* 35 (8) (2023) 1430–1462.
 - [48] Y. Goto, K. Shibata, Emergence of higher exploration in reinforcement learning using a chaotic neural network, in: *Neural Information Processing*, Springer International Publishing, Cham, 2016, pp. 40–48.
 - [49] Y. Goto, K. Shibata, Influence of the chaotic property on reinforcement learning using a chaotic neural network, in: *Neural Information Processing*, Springer International Publishing, Cham, 2017, pp. 759–767.
 - [50] K. Sato, Y. Goto, K. Shibata, Chaos-based reinforcement learning when introducing refractoriness in each neuron, in: *Robot Intelligence Technology and Applications*, Springer Singapore, Singapore, 2019, pp. 76–84.
 - [51] T. P. Lillicrap, J. J. Hunt, A. Pritzel, N. Heess, T. Erez, Y. Tassa, D. Silver, D. Wierstra, Continuous control with deep reinforcement learning, *arXiv preprint arXiv:1509.02971*.
 - [52] T. Matsuki, S. Inoue, K. Shibata, Q-learning with exploration driven by internal dynamics in chaotic neural network, in: *2020 International Joint Conference on Neural Networks (IJCNN)*, IEEE, 2020, pp. 1–7.
 - [53] S. Fujimoto, H. Hoof, D. Meger, Addressing function approximation error in actor-critic methods, in: *International conference on machine learning*, PMLR, 2018, pp. 1587–1596.
 - [54] D. Silver, G. Lever, N. Heess, T. Degris, D. Wierstra, M. Riedmiller, Deterministic policy gradient algorithms, in: *International conference on machine learning*, Pmlr, 2014, pp. 387–395.
 - [55] W. Maass, T. Natschläger, H. Markram, Real-time computing without stable states: A new framework for neural computation based on perturbations, *Neural computation* 14 (11) (2002) 2531–2560.
 - [56] H. Jaeger, The “echo state” approach to analysing and training recurrent neural networks-with an erratum note, Bonn, Germany: German National Research Center for Information Technology GMD Technical Report 148 (34) (2001) 13.
 - [57] N. Bertschinger, T. Natschläger, Real-time computation at the edge of chaos in recurrent neural networks, *Neural computation* 16 (7) (2004) 1413–1436.
 - [58] J. Boedeker, O. Obst, J. T. Lizier, N. M. Mayer, M. Asada, Information processing in echo state networks at the edge of chaos, *Theory in Biosciences* 131 (3) (2012) 205–213.
 - [59] H.-H. Chang, L. Liu, Y. Yi, Deep echo state q-network (deqn) and its application in dynamic spectrum sharing for 5g and beyond, *IEEE Transactions on Neural Networks and Learning Systems*.
 - [60] T. Matsuki, Deep q-network using reservoir computing with multi-layered readout, *arXiv preprint arXiv:2203.01465*.
 - [61] M. Beggs, John, D. Plenz, Neuronal avalanches in neocortical circuits, *Journal of neuroscience* 23 (35) (2003) 11167–11177.
 - [62] M. Beggs, John, The criticality hypothesis: how local cortical networks might optimize information processing, *Philosophical Transactions of the Royal Society A: Mathematical, Physical and Engineering Sciences* 366 (1864) (2007) 329–343.
 - [63] L. Cocchi, L. Gollo, Leonardo, A. Zalesky, M. Breakspear, Criticality in the brain: A synthesis of neurobiology, models and cognition, *Progress in neurobiology* 158 (2017) 132–152.
 - [64] J. Shi, K. Kirihara, M. Tada, M. Fujioka, K. Usui, D. Koshiyama, T. Araki, L. Chen, K. Kasai, K. Aihara, Criticality in the healthy brain, *Frontiers in Network Physiology* 1 (2022) 755685.
 - [65] Z. Tong, G. Tanaka, Reservoir computing with untrained convolutional neural networks for image

- recognition, in: 2018 24th International Conference on Pattern Recognition (ICPR), IEEE, 2018, pp. 1289–1294.
- [66] H. Chang, K. Futagami, Reinforcement learning with convolutional reservoir computing, *Applied Intelligence* 50 (8) (2020) 2400–2410.
 - [67] C. Gallicchio, A. Micheli, L. Pedrelli, Deep reservoir computing: A critical experimental analysis, *Neurocomputing* 268 (2017) 87–99.
 - [68] C. Gallicchio, A. Micheli, Echo state property of deep reservoir computing networks, *Cognitive Computation* 9 (3) (2017) 337–350.
 - [69] Q. Ma, L. Shen, G. W. Cottrell, Deep-esn: A multiple projection-encoding hierarchical reservoir computing framework, arXiv preprint arXiv:1711.05255.
 - [70] Y. Sakemi, K. Morino, T. Leleu, K. Aihara, Model-size reduction for reservoir computing by concatenating internal states through time, *Scientific reports* 10 (1) (2020) 1–13.
 - [71] K. Shibata, T. Ejima, Y. Tokumaru, T. Matsuki, Sensitivity – local index to control chaoticity or gradient globally –, *Neural Networks* 143 (2021) 436–451.
 - [72] Y. Sakemi, S. Nobukawa, T. Matsuki, T. Morie, K. Aihara, Learning reservoir dynamics with temporal self-modulation, *Communications Physics* 7 (1) (2024) 29.